EXTENDING MSC /DYTRAN FOR THE NUMERICAL SOLUTION OF THE NAVIER-STOKES EQUATIONS

Ortwin Ohtmer
Department of Mechanical Engineering
California State University, Long Beach, U.S.A.

ABSTRACT

MSC/DYTRAN contains two finite element processors, Lagrangian (finite element) and Eulerian (finite volume).

In the Eulerian processor, the grid points are fixed in space and the elements are simply partitions of the space defined by connected grid points. The Eulerian mesh is then a fixed frame of reference. The material of a body under analysis moves through the Eulerian mesh mesh and the mass, momentum, and energy of the material is transported from element to element. In ALE applications, the Eulerian gridpoints may move in space, whereby the material flows through a moving and deforming Eulerian mesh. It is important to realize that the Euler gridpoint motion is uncoupled from the material motion.

MSC/DYTRAN is efficient and extensively vectorized. It provides cost-effective solutions on the latest generation of computers ranging in size from engineering workstations to the largest supercomputers.

Based on many publications, summarized by H. Oertel Jr., the FINITE VOLUME Method, implemented in MSC/DYTRAN, is successfully applied today for the numerical fluid flow simulation. Therefore it makes sense to modify and extend MSC/DYTRAN to solve the three-dimensional NAVIER-STOKES Equations. The governing equations in integral form of conservation are applied for the computation of the compressible airfoil-flow within the FINITE VOLUME Method using MSC/DYTRAN and the menu-driven ME-Software Bank to demonstrate the numerical procedure.

1 INTRODUCTION

This paper is in parts basically a translation of the summary published in [23] by H. Oertel, Jr. The numerical fluid-flow simulation is developed as an established, reliable method in fluid mechanics comparable to results obtained in testing labs. The procedure of numerical simulation utilized by the engineer corresponds with the experimental measurements. Both methods have as an objective to solve a given fluid-flow problem as accurately as possible using the appropriate numerical or experimental proceedings. The numerical "experiment" is a technique familiar to the engineer but almost unknown to the mathematician. In particular the objective in the area of fluid-flow mechanics is the numerical solution of the three-dimensional NAVIER-STOKES Equations (conservation of mass, impulse and energy),

a system of nonlinear partial Differential Equations of second order. Their solution algorithms in regards to stability and convergence in a mathematical sense were developed only as estimates. A theory of the global existence of solutions of the compressible NAVIER-STOKES Equations could not be developed [1], [2]. Basic publications are referenced in [23] and in this paper from [1] to [22].

Nevertheless, the engineer obtains numerical approximate solutions intended to solve technical flow problems in the sense that the comparison of the numerical solution and the qualitative experiment makes up for the mathematical inaccuracy. The development of the numerical methods in fluid-mechanics started with the Finite Difference Methods, replaced later by the Finite Volume Methods, which were afterwards updated to the Adaptive Finite Element Methods for transient three-dimensional fluid-flow problems.

Parallel to those numerical procedures, the GALERKIN and Spectral Methods were developed specifically for the solution of fluid-flow stability problems. Of the numerous publications on numerical fluid-flow mechanics, only the overview of LOMAX and MEHTA are mentioned here [3].

In this paper, which is based on [4] and [23], I try to demonstrate the numerical methods applied to the laminar-turbulent transition in the compressible Boundary layer flow and the computation of the flow around a commercial aircraft airfoil. Following [4] and [23], I summarize a Spectral Method and describe the Finite Volume Method in more detail for the numerical solution of the three-dimensional compressible NAVIER-STOKES Equations. The solution for the numerical simulation of boundary layer flow transition within the Spectral method is approximated by a global Taylor Series. The governing fluid-flow Equations in integral form of conservation are applied for the computation of the compressible airfoil-flow within the Finite Volume Method. MSC/DYTRAN contains two finite element processors, Lagrangian (finite element) and Eulerian (finite volume).

In the Eulerian processor, the grid points are fixed in space and the elements are simply partitions of the space defined by connected grid points. The Eulerian mesh is then a fixed frame reference. The material of a body under analysis moves through the Eulerian mesh and the mass, momentum, and energy of the material is transported from element to element.

MSC/DYTRAN is efficient and extensively vectorized. It provides cost-effective solutions on the latest generation of computers ranging in size from engineering workstations to the largest supercomputers. Based on many publications, summarized by H. Oertel Jr., the FINITE VOLUME Method, implemented in MSC/DYTRAN, is successfully applied today for the numerical fluid flow simulation. Therefore, it makes sense to modify and extend MSC/DYTRAN to solve the three-dimensional NAVIER-STOKES Equations.

Within the following chapters the governing equations in integral form of conservation are developed and then applied for the computation of the compressible airfoil-flow within the FINITE VOLUME Method using MSC/DYTRAN and the menu-driven ME-Software Bank to demonstrate the numerical procedure.

2 FLUID FLOW SIMULATION BASIC OVERVIEW

2.0 GOVERNING EQUATIONS AND SOLUTION PROCEDURE

For the quantitative description of the fluid-flow, the values of the velocity field $\{u\}(\{x\},t)$, the pressure field $p(\{x\},t)$ and the mass density field $\rho(\{x\},t)$ must be specified at every point of the considered field at every time. For this reason the continuum mechanical governing equations are used.

2.1 NAVIER-STOKES EQUATIONS

The continuum-mechanical governing equations for the description of the conservation of the mass, impulse and the energy are given for example in the fluid mechanics II textbook [4]. The following equivalent notations are used within a Cartesian coordinate system (x,y,z).
Coordinate vector:

$$\{x\} = \begin{Bmatrix} x \\ y \\ z \end{Bmatrix} = \begin{Bmatrix} x_1 \\ x_2 \\ x_3 \end{Bmatrix} \tag{1}$$

Velocity vector:

$$\{u\} = \begin{Bmatrix} u \\ v \\ w \end{Bmatrix} = \begin{Bmatrix} u_1 \\ u_2 \\ u_3 \end{Bmatrix} \tag{2}$$

Gravity vector:

$$\{f\} = \{g\} = \begin{Bmatrix} f_1 \\ f_2 \\ f_3 \end{Bmatrix} = \begin{Bmatrix} g_x \\ g_y \\ g_z \end{Bmatrix} \tag{3}$$

Conduction heat flux vector:

$$\{q\} = \begin{Bmatrix} q_1 \\ q_2 \\ q_3 \end{Bmatrix} = \begin{Bmatrix} q_x \\ q_y \\ q_z \end{Bmatrix} \tag{4}$$

Stress Tensor $\sigma_{ij} = \tau_{ij}$ written in matrix notation $[\tau]$
(Note: i and j are the corresponding columns and rows)

$$[\tau] = \begin{bmatrix} \sigma_{xx} & \sigma_{xy} & \sigma_{xz} \\ \sigma_{xy} & \sigma_{yy} & \sigma_{yz} \\ \sigma_{xz} & \sigma_{yz} & \sigma_{zz} \end{bmatrix} = \begin{bmatrix} \tau_{11} & \tau_{12} & \tau_{13} \\ \tau_{21} & \tau_{22} & \tau_{23} \\ \tau_{31} & \tau_{32} & \tau_{33} \end{bmatrix} \tag{5}$$

Surface force vector {P}

$$\{P\} = \begin{Bmatrix} P_x \\ P_y \\ P_z \end{Bmatrix} = \frac{\partial\{p_x\}}{\partial x} + \frac{\partial\{p_y\}}{\partial y} + \frac{\partial\{p_z\}}{\partial z} \tag{6}$$

where

$$\{p_x\} = \begin{Bmatrix} \tau_{xx} \\ \tau_{xy} \\ \tau_{xz} \end{Bmatrix}; \{p_y\} = \begin{Bmatrix} \tau_{xy} \\ \tau_{yy} \\ \tau_{yz} \end{Bmatrix}; \{p_z\} = \begin{Bmatrix} \tau_{xz} \\ \tau_{yz} \\ \tau_{zz} \end{Bmatrix}$$

The stress vectors $\{p_x\}$; $\{p_y\}$; $\{p_z$ are the rows or columns of the stress tensor τ_{ij} or $[\tau]$.

Conservation of mass:

$$\frac{\partial\rho}{\partial t} + \frac{\partial(\rho u)}{\partial x} + \frac{\partial(\rho v)}{\partial y} + \frac{\partial(\rho w)}{\partial z} = 0 \tag{7}$$

In tensor notation:

$$\frac{\partial\rho}{\partial t} + \frac{\partial(\rho u_i)}{\partial x_i} = 0 \tag{8}$$

Conservation of impulse: (Equations (9), (10), (11))

$$\frac{\partial(\rho u)}{\partial t} + \rho\left(u\frac{\partial u}{\partial x} + v\frac{\partial u}{\partial y} + w\frac{\partial u}{\partial z}\right) + \frac{\partial p}{\partial x} - \left(\frac{\partial\tau_{xx}}{\partial x} + \frac{\partial\tau_{xy}}{\partial y} + \frac{\partial\tau_{xz}}{\partial z}\right) - \rho f_x = 0 \tag{9}$$

$$\frac{\partial(\rho v)}{\partial t} + \rho\left(u\frac{\partial v}{\partial x} + v\frac{\partial v}{\partial y} + w\frac{\partial v}{\partial z}\right) + \frac{\partial p}{\partial y} - \left(\frac{\partial\tau_{xy}}{\partial x} + \frac{\partial\tau_{yy}}{\partial y} + \frac{\partial\tau_{yz}}{\partial z}\right) - \rho f_y = 0 \tag{10}$$

$$\frac{\partial(\rho w)}{\partial t} + \rho(u\frac{\partial w}{\partial x} + v\frac{\partial w}{\partial y} + w\frac{\partial w}{\partial z}) + \frac{\partial p}{\partial z} + (\frac{\partial \tau_{xz}}{\partial x} + \frac{\partial \tau_{yz}}{\partial y} + \frac{\partial \tau_{zz}}{\partial z}) - \rho f_z = 0 \qquad (11)$$

In tensor notation:

$$\frac{\partial(\rho u_j)}{\partial t} + \rho(u_i\frac{\partial u_j}{\partial x_i}) + \frac{\partial p}{\partial x_j} - \frac{\partial \tau_{ji}}{\partial x_i} - \rho f_j = 0 \qquad (12)$$

Conservation of energy:

$$\rho(\frac{\partial e}{\partial t} + u\frac{\partial e}{\partial x} + v\frac{\partial e}{\partial y} + w\frac{\partial e}{\partial z}) - \frac{p}{\rho}(\frac{\partial \rho}{\partial t} - u\frac{\partial \rho}{\partial x} - v\frac{\partial \rho}{\partial y} + w\frac{\partial \rho}{\partial z})$$

$$- \tau_{xx}\frac{\partial u}{\partial x} - \tau_{xy}\frac{\partial v}{\partial x} - \tau_{xz}\frac{\partial w}{\partial x} - \tau_{xy}\frac{\partial u}{\partial y} - \tau_{yy}\frac{\partial v}{\partial y} - \tau_{yz}\frac{\partial w}{\partial y}$$

$$- \tau_{xz}\frac{\partial u}{\partial z} - \tau_{yz}\frac{\partial v}{\partial z} - \tau_{zz}\frac{\partial w}{\partial z} + \frac{\partial q_x}{\partial x} + \frac{\partial q_y}{\partial y} + \frac{\partial q_z}{\partial z} = 0 \qquad (13)$$

In tensor notation:

$$\rho(\frac{\partial e}{\partial t} + u_i\frac{\partial e}{\partial x_i}) - \frac{p}{\rho}(\frac{\partial \rho}{\partial t} + u_i\frac{\partial \rho}{\partial x_i}) - \tau_{ij}\frac{\partial u_i}{\partial x_j} + \frac{\partial q_j}{\partial x_j} = 0 \qquad (14)$$

where

$$\rho\frac{\partial e}{\partial t} = \frac{\partial(e\rho)}{\partial t} = e\frac{\partial \rho}{\partial t} + \frac{\partial e}{\partial t}\rho$$

and $e = \frac{-p}{\rho}$

In addition to the five equations of conservation, the governing equations for the specific inner energy e and the temperature T must be considered to be able to calculate all unknowns, that is $e = e(p,\rho)$; $T = T(p,\rho)$

The shear stress components τ_{ij} are calculated via the NEWTON and

STOKES shear stress hypothesis and the dynamic viscosity $\mu(p,\rho)$:

$$\tau_{xx} = 2\mu(p,\rho)\frac{\partial u}{\partial x} \qquad (15)$$

$$\tau_{yy} = 2\mu(p,\rho)\frac{\partial v}{\partial y} \qquad (16)$$

$$\tau_{zz} = 2\mu(p,\rho)\frac{\partial w}{\partial z} \tag{17}$$

$$\tau_{xy} = \mu(p,\rho)(\frac{\partial u}{\partial y} + \frac{\partial v}{\partial x}) \tag{18}$$

$$\tau_{yz} = \mu(p,\rho)(\frac{\partial v}{\partial z} + \frac{\partial w}{\partial y}) \tag{19}$$

$$\tau_{xz} = \mu(p,\rho)(\frac{\partial w}{\partial x} + \frac{\partial u}{\partial z}) \tag{20}$$

In tensor notation:

$$\tau_{ij} = -\frac{2}{3}\mu(p,\rho)\frac{\partial u_i}{\partial x_i}\delta_{ij} + \mu(p,\rho)(\frac{\partial u_i}{\partial x_j} + \frac{\partial u_j}{\partial x_i}) \tag{21}$$

where $\delta_{ij} = 1$ for i=j or $\delta_{ij} = 0$ for $i \neq j$

The average pressure $\bar{p}$ is defined as:

$$\bar{p} = -\frac{1}{3}\tau_{ii} = -\frac{1}{3}(\tau_{11} + \tau_{22} + \tau_{33})$$

$$\bar{\mu} = -\frac{2}{3}\mu \quad \text{where } \mu^* = \frac{1}{2}\mu$$

$\bar{\mu}$ and μ^* are the Lame' constants in the theory of elasticity. $G = \mu$ is named the shear modulus.

The conduction heat flux vector {q} is computed via the Fourier equation

of thermal conductivity with the thermal conductivity coefficient $\lambda(p,\rho)$.

$$\{q\} = -\lambda(p,\rho)\nabla T \tag{22}$$

where

$$\{q\} = \begin{Bmatrix} q_x \\ q_y \\ q_z \end{Bmatrix} \text{ and } \nabla T = \begin{Bmatrix} \frac{\partial T}{\partial x} \\ \frac{\partial T}{\partial y} \\ \frac{\partial T}{\partial z} \end{Bmatrix}$$

In tensor notation: $q_i = -\lambda(p,\rho)\frac{\partial T}{\partial x_i}$ (23)

The dynamic governing equations for viscous fluids can be summarized as Newton Law in vector notation.

$$\rho\frac{d\{u\}}{dt} = \rho\{g\} + \{P\} \quad (24)$$

In (24), $\rho\{g\}$ is the weight per volume and $\{P\}$ is the surface force vector of the volume element consisting of forces (pressure) in the normal direction and shear forces in tangential direction of the surfaces.

The the velocity vector $\{u\}$, the gravity vector $\{g\}$ and the surface force vector $\{P\}$ are specified in equations (2), (3) and (6). $\{P\}$ is the resultant surface force per volume. A graphical representation of the surface stresses of one volume element $dV = dx\,dy\,dz$ is shown in figure 1.

The specified differential equations together with initial and boundary conditions specify a specific boundary value problem and its unique solution. As a fluid dynamics example, the fluid flow around a wing of an aircraft is considered. The boundary conditions specify a zero velocity at the surface of the wing and the undisturbed velocity at infinity. For the simulation of the laminar-turbulent transition, the stationary laminar fluid is assumed as the initial condition with a draining wave disturbance (Tollmien-Schlichting wave) as well as an overlaid small amplitude diagonal wave disturbance. According to the physical model, periodic boundary conditions are such that there is zero velocity at the wall. At large distances from the wall, the draining wave disturbances are less distinct.

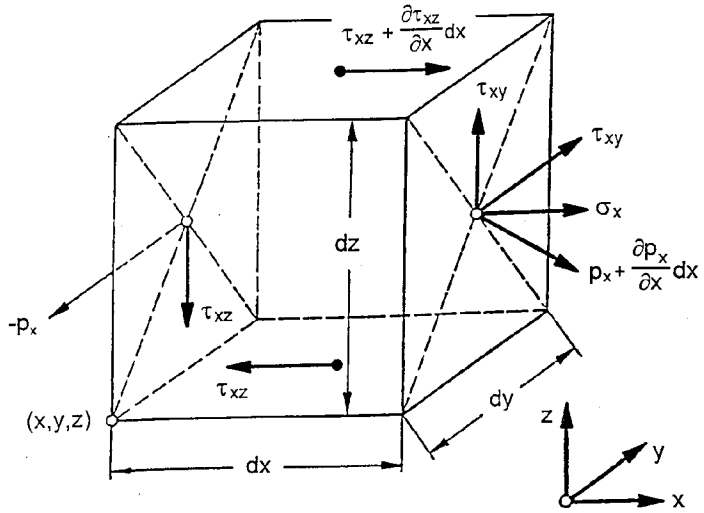

Figure 1
Stress tensor for viscous flow

2.1.1 NAVIER-STOKES EQUATION IN CONSERVATIVE FORM

For the application of the Spectral and Finite Volume methods, the Navier-Stokes equations are specified in conservative form because this notation is very suitable in numerical fluid dynamics. In contrast to the notation in primitive variables, the stable and smooth solutions are still obtained via the conservative formulation even if discontinuities occur in the flow field. An example would be condensation shock. Deriving the governing equations within a fixed global control volume, the conservative formulation is obtained while the primitive variables formulation is based on a local moving control volume.

The conservative formulation of the Navier-Stokes equations is characterized by the fact that every single equation of mass, impulse and energy conservation has a divergence term which permits the vector notation of the Navier-Stokes equations to specify column vectors and add them together into one vector equation. This is possible due to the following simplifications:
The first four terms in equations (9), (10) and (11) can be rewritten as:

$$\frac{\partial(\rho u)}{\partial t} + \rho(u\frac{\partial u}{\partial x} + v\frac{\partial u}{\partial y} + w\frac{\partial(u)}{\partial z}) = \tag{25}$$

$$\frac{\partial(\rho u)}{\partial t} + \rho(\frac{\partial(u^2)}{\partial x} + \frac{\partial(uv)}{\partial y} + \frac{\partial(uw)}{\partial z}) =$$

$$\frac{\partial \rho}{\partial t}u + \rho\frac{\partial u}{\partial t} + \rho(2u\frac{\partial u}{\partial x} + u\frac{\partial v}{\partial y} + v\frac{\partial u}{\partial y} + u\frac{\partial w}{\partial z} + w\frac{\partial u}{\partial z}) \tag{26}$$

with

$$u(\frac{\partial \rho}{\partial t} + \rho(\frac{\partial u}{\partial x} + \frac{\partial v}{\partial y} + \frac{\partial w}{\partial z})) = 0$$

representing the equation (7); because u is a non zero value
$(\frac{\partial \rho}{\partial t} + \rho(\frac{\partial u}{\partial x} + \frac{\partial v}{\partial y} + \frac{\partial w}{\partial z}) = 0.$

The five NAVIER-STOKES equations can be rewritten in the following conservative form of one vector equation.

$$\frac{\partial\{U\}}{\partial t} + \frac{\partial\{F\}}{\partial x} + \frac{\partial\{G\}}{\partial y} + \frac{\partial\{H\}}{\partial z} = 0 \tag{27}$$

or

$$\frac{\partial\{U\}}{\partial t} + \text{div}\,[R] = 0 \tag{28}$$

with
$[R] = [\{F\}, \{G\}, \{H\}]$

and

$$\{U\} = \begin{Bmatrix} \rho \\ \rho u \\ \rho v \\ \rho w \\ \rho e_{tot} \end{Bmatrix}$$

$$\{F\} = \begin{Bmatrix} \rho u \\ \rho u^2 + p - \tau_{xx} \\ \rho vu - \tau_{xy} \\ \rho wu - \tau_{xz} \\ (\rho e_{tot} + p - \tau_{xx})u - \tau_{xy}v - \tau_{xz}w - \lambda\frac{\partial T}{\partial x} \end{Bmatrix}$$

$$\{G\} = \begin{Bmatrix} \rho v \\ \rho uv - \tau_{yx} \\ \rho v^2 - \tau_{yy} \\ \rho wv - \tau_{yz} \\ (\rho e_{tot} + p - \tau_{yy})v - \tau_{yz}w - \tau_{yx}u - \lambda\frac{\partial T}{\partial y} \end{Bmatrix}$$

$$\{H\} = \begin{Bmatrix} \rho w \\ \rho uw - \tau_{xz} \\ \rho vw - \tau_{zy} \\ \rho w^2 + p - \tau_{zz} \\ (\rho e_{tot} + p - \tau_{zz})w - \tau_{zx}u - \tau_{zy}v - \lambda\frac{\partial T}{\partial z} \end{Bmatrix}$$

Historically the Navier-Stokes equations were specifying the impulse equations for one fluid element. In the modern literature of numerical fluid mechanics, the Navier-Stokes equations are named in an expanded sense describing the whole system of equations for a fluid problem.

2.1.2 DIMENSIONLESS NAVIER-STOKES EQUATIONS IN CONSERVATIVE FORM

In general, dimensionless coefficients are preferred in fluid mechanics to be able to convert the variables of one specific flow field into another. Since in numerical fluid mechanics the solutions of a system of differential equations are not analytic functions but real values, it seems to be obvious to introduce dimensionless coefficients. First, the Cartesian coordinates {x} are made dimensionless via a characteristic length L of the whole flow field. The dimensionless variables are indicated with an asterisk *.

$$\{x^*\} = \frac{\{x\}}{L} \tag{29}$$

The components of the velocity vector {u} are divided by the constant flow velocity at infinity U_∞ to obtain dimensionless velocity.

$$\{u^*\} = \frac{\{u\}}{U_\infty} \tag{30}$$

For dimensionless time:

$$t^* = \frac{t\, U_\infty}{L} \tag{31}$$

Additionally dimensionless values are needed for mass density ρ,

$$\rho^* \frac{\rho}{\rho_\infty} \tag{32}$$

pressure p,

$$p^* = \frac{p}{p_\infty U_\infty^2} \tag{33}$$

temperature T,

$$T^* = \frac{T}{T_\infty} \tag{34}$$

dynamic viscosity μ,

$$\mu^* = \frac{\mu}{\mu_\infty} \tag{35}$$

and thermal conductivity λ,

$$\lambda^* = \frac{\lambda}{\lambda_\infty} \tag{36}$$

Dimensionless values are also needed for specific total energy e_{tot} per volume

$$e^*_{tot} = \frac{e_{tot}}{p_\infty c_{p\infty} T_\infty} \tag{37}$$

The stress tensor τ_{ij} can be written in the following dimensionless notation:

$$\tau^*_{ij} = \mu^*\left(\frac{\partial u^*_i}{\partial x^*_j} + \frac{\partial u^*_j}{\partial x^*_i}\right) - \frac{2}{3}\mu^* \frac{\partial u^*_i}{\partial x^*_i}\,\delta_{ij} \tag{38}$$

It is also convenient to introduce the following characteristic parameters.

$$\text{Reynolds number } Re = \frac{U_\infty L_\infty \rho_\infty}{\mu_\infty} \tag{39}$$

$$\text{Prandtl number } Pr = \frac{\mu_\infty c_{p_\infty}}{\lambda_\infty} \tag{40}$$

$$\text{Mach number } M_\infty = \frac{U_\infty}{a_\infty} \tag{41}$$

Inserting the dimensionless parameters in equation (27), the dimensionless conservative form of the Navier-Stokes equations are obtained.

Two basic numerical methods are applied to solve the dimensionless conservative Navier-Stokes equations. These are the spectral and the finite volume methods.

A constant acceleration vector {a} is selected for each volume element of a fine mesh for the Finite Volume Method while within the Spectral Method a Fourier Analysis in two or three dimensions is performed on the entire surface of a wing.

2.2 REYNOLDS EQUATIONS IN CONSERVATIVE FORM

Fluids in physics and engineering exist in two different fundamental shapes and patterns; the laminar flow and the turbulent flow. Based on a macroscopic observation of the fluid particles, the laminar fluid elements move in parallel layers while the turbulent fluid elements move not only in the mainstream direction but also oscillate perpendicular to the mainstream movement. A staggering (waving) velocity is superimposed perpendicular to the mainstream velocity, named turbulent flow. The switch from laminar to turbulent flow causes effects comparable to a multiple increase in fluid viscosity. Due to the extraordinary complexity of staggering fluid movement, up to now theoretical computations of turbulent flows are not possible. In engineering applications the details of movements perpendicular to the mainstream velocity are not so important to know therefore results are obtained by averaging the turbulent movement over a time period.

2.2.1 TIME-DEPENDENT AVERAGING

The Reynolds description of turbulent flow is based on the concept of subdividing all time dependent unknown parameters $\Phi(x,y,z,t)$ in time dependent average values $\bar{\Phi}(x,y,z,t)$ and time dependent fluctuation values $\Phi^*(x,y,z,t)$ defined as follows:

$$\Phi(x,y,z,t) = \bar{\Phi}(x,y,z,t) + \Phi^*(x,y,z,t) \tag{42}$$

where

$$\bar{\Phi}(x,y,z,t) = \frac{1}{T}\int_0^T \Phi(x,y,z,t+\tau)d\tau$$

The time period T should be selected, so that an increasing T is nearly not changing the value of $\bar{\Phi}$. In other words the selected T value is larger than the average time period of the oscillating values of Φ^*. The definition of the time dependent average value $\bar{\Phi}$ requires that the time dependent average fluctuation value $\bar{\Phi}^*$ is zero ($\bar{\Phi}^*(x,y,z,t) = 0$).

For compressible flow, a simplification can be obtained by specifying mass density ρ to related average values $\tilde{\Phi}$.

$$\Phi(t) = \tilde{\Phi} + \Phi^{**} \tag{43}$$

where

$$\tilde{\Phi} = \frac{1}{\bar{\rho}\,T}\int_0^T \rho(t+\tau)\,\Phi(t+\tau)d\tau$$

Inserting the specified average field parameters in the compressible Navier-Stokes equations the "average" mass, impulse and energy conservation equations can be written as in [23].

The additional terms with staggering components, indicated via asterisks, are unknown as well as the averaged parameters over specific time period indicated by (T bar) $\bar{T} = T$. The main goal is to calculate the "bar" unknowns.

The nonlinear system of equations in integral form is not closed because it consists of more unknowns that equations. The next step is therefore to close the system of Reynolds equations. This task can be accomplished by developing a turbulence model via measurements or theoretical assumptions to specify the staggering unknown components first and then calculating the closed nonlinear system of equations.

2.2.2 FINITE VOLUME METHOD APPLIED FOR THE REYNOLDS EQUATIONS

For the calculation of the turbulent flow around a wing, a Finite Volume Method is selected to numerically solve the compressible Navier-Stokes equations in the integral form. The Finite Volume Methods can be subdivided in explicit and implicit numerical procedures, whether the discrete unknown parameters can be calculated separately in every time step (explicit diagonal mass matrix) or whether the solution of a linear system of equations in every time step is required (implicit symmetric stiffness matrix, Finite Element Method). Based on the application of the vector processors, the explicit Runge-Kutta Finite Volume Method is applied.

The flow field is subdivided in elements (cells) according to Figure **2**. At each center point of a 3D element the mathematical relations for the unknown field parameters are specified. The center points of the elements can be located by subscripts i, j, k in space, indicating the x, y, z directions.

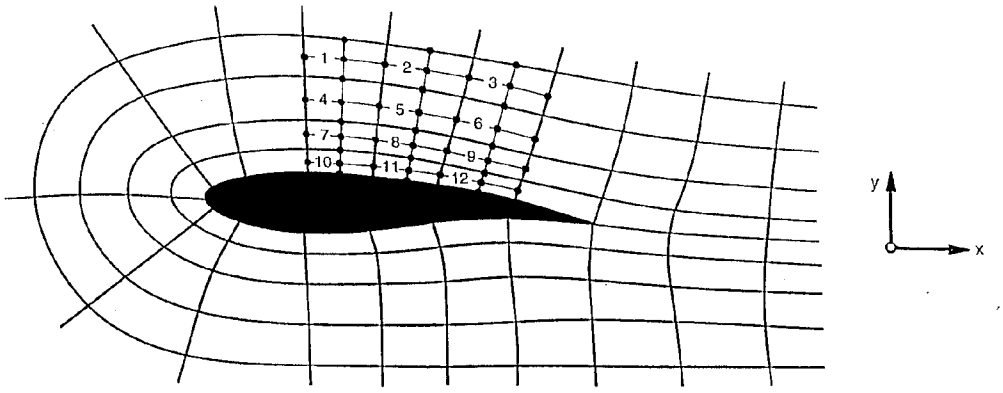

Figure **2**
Finite volume element center points connectivity visualization via straight lines

Based on the definition of the Reynolds equations on the previous pages, the related integral form is applied for each element (volume). The volume integrals of an element for the first derivatives of the flux vectors :

$\frac{\partial}{\partial x}\{F\}$, $\frac{\partial}{\partial y}\{G\}$ and $\frac{\partial}{\partial z}\{H\}$ are transformed to surface integrals via the Gauss Integral Theorem resulting in the following vector equations:

$$\frac{\partial\{U\}}{\partial t} = -\text{div}\,[R] \qquad (44)$$

where

$[R] = [\{F\}, \{G\}, \{H\}]$

and

$$\int_V \text{div}\,[R]\,dV = \int_S [R]^T \{n\}\,dS$$

and

$\{n\} = \begin{Bmatrix} n_x \\ n_y \\ n_z \end{Bmatrix}$ is the outer unit normal vector of the closed surface S of an element

The conservation vector equation for an element can therefore be rewritten as:

$$\frac{\partial}{\partial t}\int_{V_{element}} \{U\}dV = -\int_{S_{element}} \{\{F\}\,n_x + \{G\}\,n_y + \{H\}\,n_z\}\,dS \qquad (45)$$

The integration over all volume elements fulfills the equilibrium equations within each element while the flux vectors {F}, {G} and {H} in the x, y and z direction at the surfaces of the elements intersect with the surfaces of the adjacent volume elements.

The standard Finite Element Assembly in matrix notation can therefore be applied to specify the system of equations for the flow field. The volume cells specified as brick elements have six plane surfaces. When flux vectors are specified, it is assumed that the distributed mass within a cell is concentrated as a point mass at the center of the volume cell. This is shown in Figure 3.

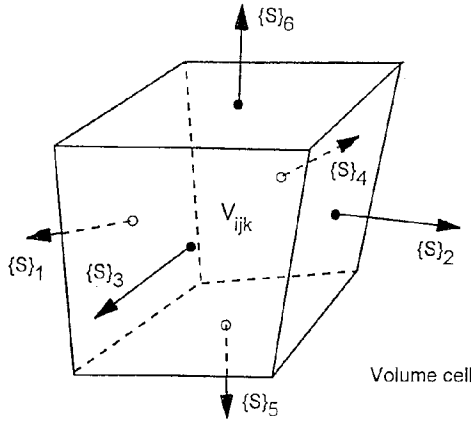

Figure 3
Volume cell and normal vectors

The plane surfaces of a volume cell are oriented via their outer normal vectors $\{n\}_l$ multiplied by the associated surface area S_l: that is $\{S\}_l = S_l \{n\}_l$. The flux vectors are defined in a global coordinate system. For arbitrary oriented volume elements in space, the x, y, z components can easily be specified by standard coordinate transformations. Symbolically the governing equation set for one volume element can be defined as follows:

$$\frac{d}{dt}\{U_{ijk}\} V_{ijk} + \sum_{l=1}^{6} \{\{F_{(l)}\} + \{G_{(l)}\} + \{H_{(l)}\}\} S_{(l)}\}_{ijk} = 0 \qquad (46)$$

where

$$\{F_{(l)}\}S_l = \{F_{(l)} S_l \quad : l \in 1,2\}$$
$$\{F_{(l)}\}S_l = \{\ 0 \quad : l \in 3, 4, 5, 6\}$$

$$\{G_{(l)}\}S_l = \{G_{(l)} S_l \quad : l \in 3,4\}$$
$$\{G_{(l)}\}S_l = \{\ 0 \quad : l \in 1, 2, 5, 6\}$$

$$\{H_{(l)}\}S_l = \{H_{(l)} S_l \quad : l \in 5,6\}$$
$$\{H_{(l)}\}S_l = \{\ 0 \quad : l \in 1, 2, 3, 4\}$$

The start of the vectors $\{F_{(l)}\}$, $\{G_{(l)}\}$, and $\{H_{(l)}\}$ is located at the center points of the surfaces of a volume element. Each vector is overlapping with its counterpart of the adjacent surface part of the adjacent volume element specifying the assembly of all equations in global coordinates. Selecting a fine mesh structure, the unknown field parameters $u^{(i)}$ specifying the surface vectors $\{F_{(l)}\}$, $\{G_{(l)}\}$, and $\{H_{(l)}\}$ can be approximated by the unknown field parameters at adjacent center points of volume elements $u_{i,j,k}$ as shown in (47).

$$u^{(1)} = \frac{1}{2}(u_{i,\,j-1,\,k} + u_{i,\,j,\,k}$$

$$u^{(2)} = \frac{1}{2}(u_{i-1,\,j,\,k} + u_{i,\,j,\,k}$$

$$u^{(3)} = \frac{1}{2}(u_{i,\,j+1,\,k} + u_{i,\,j,\,k}$$

$$u^{(4)} = \frac{1}{2}(u_{i,\,j-1,\,k} + u_{i,\,j,\,k}$$

$$u^{(5)} = \frac{1}{2}(u_{i,\,j,\,k-1} + u_{i,\,j,\,k}$$

$$u^{(6)} = \frac{1}{2}(u_{i,\,j,\,k+1} + u_{i,\,j,\,k} \qquad (47)$$

Equation (46) is only valid if all three dimensional volume elements (figure 3) have a rectangular shape. For an arbitrary surface in space, the normal direction has non zero components in the x, y, z directions. These shapes are considered in MSC/DYTRAN. The topology of the volume elements are specified via the element incidence's commonly used for finite element input. The surfaces of the eight, six and four noded solid elements are based on the node numbering as shown in figure 4.

Eight noded Solid-Element:

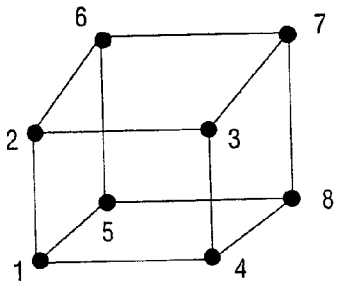

Face Number	Grid Points
1	1432
2	1265
3	1584
4	7856
5	7348
6	7623

Six noded Solid-Element :

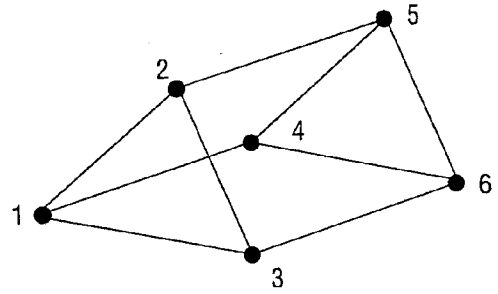

Face Number	Grid Points
1	132
2	1254
3	1463
4	645
5	6523

Four noded Solid-Element :

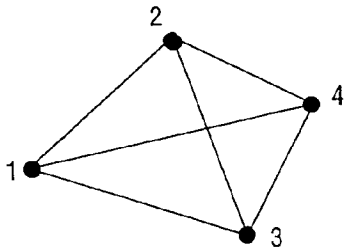

Face Number	Grid Points
1	132
2	124
3	143
4	423

figure 4 DYTRAN shapes

Finally we can specify a system of nonlinear ordinary differential equations specifying the fluid flow boundary value problem.

$$\frac{d}{dt}\{U_{ijk}\} = -\{Q(\{U_{ijk}\})\} \tag{48}$$

where $\{Q(\{U_{ijk}\})\}$ is the discretization operator.

The last vector equation can be rewritten in matrix notation based on Finite Element concepts.

$$[V]_r \{\frac{d}{dt} U\}_r = - [P(\{U\})][S]^h_r \{J\}_r \tag{49}$$

with

$$\{U\}^T = \{\{U_1\}^T, \{U_2\}^T, \{U_3\}^T, \ldots \{U_n\}^T$$

$$\{U_i\}^T = \{\rho_i, \rho_i u_i, \rho_i v_i, \rho_i w_i, \rho_i e_{tot}\}$$

$$[P] = \frac{1}{2}[\{F\}_1, \{G\}_1, \{H\}_1, \{F\}_2, \{G\}_2, \{H\}_2, \ldots . \{F\}_n, \{G\}_n, \{H\}_n]$$

where n is the number of volume elements (cells)

The subscripts r, h = 1, 2, 3 ··· n, with n = number of elements. The subscripts r and h specify the element number and the hypercolumn number of the matrix [S], respectively. The values of the matrix [P] are only multiplied with values of a hypercolumn of the matrix [S] within the bandwidth of [S]. (The values outside the bandwidth are all zero.)

$$\{J\}^T = \{1, 1, 1, \ldots . 1\}$$

$$m = \sum_{i=1}^{n} k_i \tag{50}$$

where m is the size of vector {J} and k_i is number of surfaces or faces per element.

$$[V] = \begin{bmatrix} v_1 & & & & & & 0 \\ & v_1 & & & & & \\ & & v_1 & & & & \\ & & & v_1 & & & \\ & & & & v_1 & & \\ & & & & & v_n & \\ & & & & & & v_n \\ & & & & & & & v_n \\ & & & & & & & & v_n \\ 0 & & & & & & & & & v_n \end{bmatrix} \tag{51}$$

The matrix [S] (51) specifies the topology of the mesh and the sizes of the surfaces (figure 5)

The definition of the submatices $[S_i]$ and $[S_{ij}]$ in (51) and (52) are explained for the first two eight noded elements in figures 6 and 2. The element incidences of element 1 are 1, 2, 3, 4, 5, 6, 7, 8. The element incidences of element 2 are 4, 3, 9, 10, 8, 7, 11, 12. Both elements 1 and 2 have the surface 7,3,4,8 (face 5 of element 1 and face 2 of element 2) in common. Based on (4) the submatrices $[S_1]$, $[S_2]$, $[S_{12}]$ and $[S_{21}]$ are specified as follows: $[S_i]$ (e.g. $[S_1]$, $[S_2]$) is a single element volume where i is the element number. These elements lie on the main diagonal of matrix [S] (51).

$$[S] = \begin{array}{c} \begin{array}{cccccccccccc} 1 & 2 & 3 & 4 & 5 & 6 & 7 & 8 & 9 & 10 & 11 & 12 \end{array} \\ \begin{bmatrix} [S_1] & [S_{12}] & & [S_{14}] & & & & & & & & \\ [S_{21}] & [S_2] & [S_{23}] & & [S_{25}] & & & & & & & \\ & [S_{32}] & [S_3] & & & [S_{36}] & & & & & & \\ [S_{41}] & & & [S_4] & [S_{45}] & & [S_{47}] & & & & & \\ & [S_{52}] & & [S_{54}] & [S_5] & [S_{56}] & & [S_{58}] & & & & \\ & & [S_{63}] & & [S_{65}] & [S_6] & & & [S_{69}] & & & \\ & & & [S_{74}] & & & [S_7] & [S_{78}] & & [S_{710}] & & \\ & & & & [S_{85}] & & [S_{87}] & [S_8] & [S_{89}] & & [S_{811}] & \\ & & & & & [S_{96}] & & [S_{98}] & [S_9] & & & [S_{912}] \\ & & & & & & [S_{107}] & & & [S_{10}] & & \\ & & & & & & & [S_{118}] & & & [S_{11}] & \\ & & & & & & & & [S_{129}] & & & [S_{12}] \end{bmatrix} \end{array} \begin{array}{c} 1 \\ 2 \\ 3 \\ 4 \\ 5 \\ 6 \\ 7 \\ 8 \\ 9 \\ 10 \\ 11 \\ 12 \end{array} \quad (51)$$

Figure 5

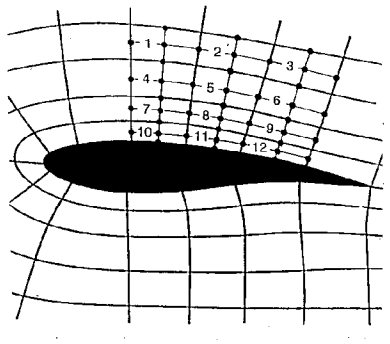

Figure 2
Finite volume element center points connectivity visualization via straight lines

$$[S]_1 = \begin{array}{c} \begin{array}{cccccc} 1 & 2 & 3 & 4 & 5 & 6 \end{array} \\ \begin{bmatrix} S_1 n_{x_1} & S_2 n_{x_2} & S_3 n_{x_3} & S_4 n_{x_4} & S_5 n_{x_5} & S_6 n_{x_6} \\ S_1 n_{y_1} & S_2 n_{y_2} & S_3 n_{y_3} & S_4 n_{y_4} & S_5 n_{y_5} & S_6 n_{y_6} \\ S_1 n_{z_1} & S_2 n_{z_2} & S_3 n_{z_3} & S_4 n_{z_4} & S_5 n_{z_5} & S_6 n_{z_6} \end{bmatrix} \end{array}$$

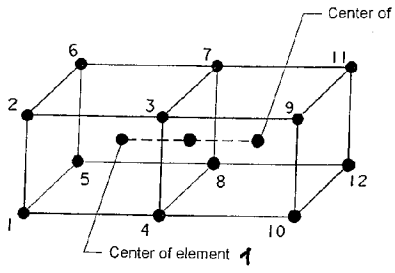

(52)

$$[S]_{21} = \begin{bmatrix} 0 & 0 & -S_2 n_{x_2} & 0 & 0 & 0 \\ 0 & 0 & -S_2 n_{y_2} & 0 & 0 & 0 \\ 0 & 0 & -S_2 n_{z_2} & 0 & 0 & 0 \end{bmatrix} \quad [S]_{12} = \begin{bmatrix} 0 & 0 & 0 & 0 & -S_5 n_{x_5} & 0 \\ 0 & 0 & 0 & 0 & -S_5 n_{y_5} & 0 \\ 0 & 0 & 0 & 0 & -S_5 n_{z_5} & 0 \end{bmatrix}$$

Fig. 6 Connectivity of elements 1 and 2

where $[S]_i = [S]_1$ for element 1

S_k = surface area of face k (k = 1 to 6 columns; there are six faces on element 1)

n_{x_k}, n_{y_k}, n_{z_k} = the x, y, z components of the outer normal unit vector of face k

The submatrices $[S_{ij}]$ represent specific element volumes that share common surfaces with other elements. It should be noted that $[S_{ij}] \neq [S]_{ji}$. The first subscript i is the element number that shares the surface with element j. These submatrices lie on both sides of the main diagonal. Referring back to figure 6, the submatrices for element 1 and 2 are defined respectively.

At the free surfaces of the elements the field parameters are zero or given values at infinity ; (n_x), (n_y) and (n_z) are the x, y, z components of the normal vectors of the element surfaces. The vector $\{U\}_i$ is an unknown field vector at the center point of the volume element i. The joint coordinates of the corner points together with the element incidence's (topology) of the given shape idealization (figure 2) are applied to calculate the center points of the elements, surfaces, sides and centers. The free surfaces as well as the surfaces adjacent to the elements can be visualized by lines connecting adjacent center points of elements (figure 6). The nonlinear system of equations has five degrees of freedom per center point. The nonlinear system of ordinary first order differential equations can be solved numerically via the standard explicit Runge-Kutta method of forth order.

The time discretization is based on equidistant time steps Δt

$$t = n\Delta t \tag{53}$$

Based on the assumption that all field parameters {U} are known before and at time $t = n\,\Delta t$, the system (49) can be integrated (differentiated) within the next time step Δt following the Runge-Kutta numerical procedure.

$$\{U^{(0)}\} = \{U^n\}$$

$$\{U^{(1)}\} = \{U^{(0)}\} - \frac{\Delta t}{2}\{Q(\{U^{(0)}\})\}$$

$$\{U^{(2)}\} = \{U^{(0)}\} - \frac{\Delta t}{2}\{Q(\{U^{(1)}\})\} \tag{54}$$

$$\{U^{(3)}\} = \{U^{(0)}\} - \frac{\Delta t}{2}\{Q(\{U^{(2)}\})\}$$

$$\{U^{(4)}\} = \{U^{(0)}\} - \frac{\Delta t}{6}\{\{Q\{U^{(0)}\}\} + 2\{Q\{U^{(1)}\}\} + 2\{Q\{U^{(2)}\}\} + \{Q\{U^{(3)}\}\}\}$$

The values calculated after the time step Δt are named $\{U^{n+1}\} = \{U^{(4)}\}$

The calculation of transonic fluids around a wing via the Finite Volume Method is relatively insensitive due to the inconsistent three dimensional mesh generations. Another advantage is the straight forward coding of the numerical procedure and the assembling of the nonlinear equation set.

2.3 STANDARD TURBULENCE MODELS

In chapter 2.2 the Reynolds equations were developed. The terms with time dependent average values of the staggering parameters could be interpreted as components of a stress tensor. This interpretation alone is not able to reduce the number of Reynolds equation unknowns. It is necessary to specify a relation between the staggering values and the average movement of the fluid. This can only be accomplished empirically via experiments. This task is named the development of a turbulence model.

3. Engineering Software Program Bank (ESP-Bank)

MSC/NASTRAN, SDRC-I-DEAS, MSC/EMAS, MSC/DYTRAN unconstrained and constrained optimization codes can easily be executed via the SYSTEM-function in C-language, and then applied within an iteration procedure. Via the NASTRAN-OUTPUT 2-file, I-DEAS and NASTRAN are linked together. The Mechanical Engineering Program-Bank provides the environment for a large variety of complex engineering problems.

Today, nearly all areas of expertise in engineering are covered via large application software packages. To integrate them all into one black box makes no sense, due to modern parallel processing technology and the need for applied research and maintenance. Therefore, we try to adapt all software systems via standards used for the pre and postprocessing of data. To run an automatic process chain, applying different software systems can easily be achieved when programming in C-language.

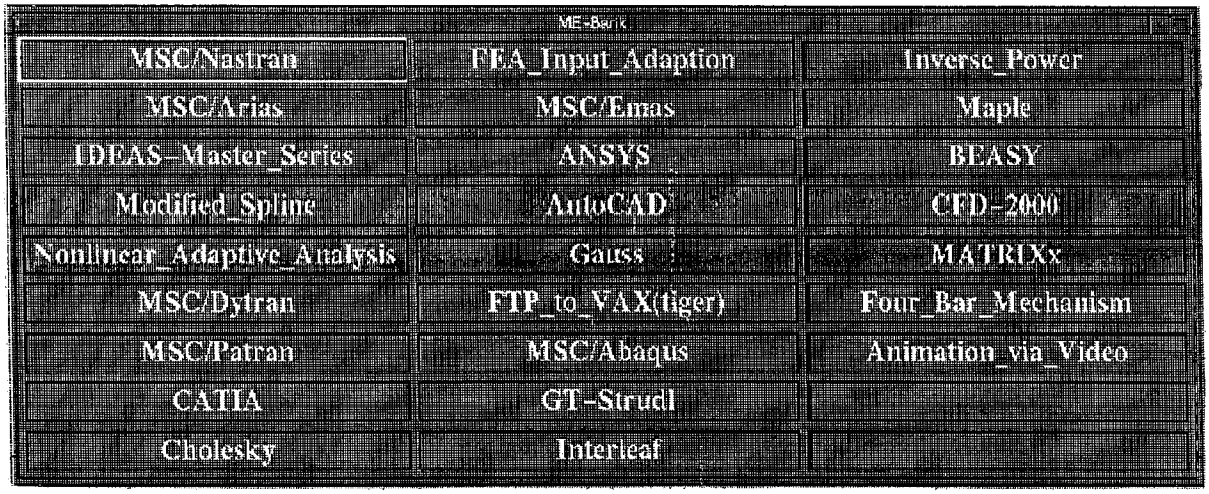

4. CONCLUSION

Via a Programbank, universities and research institutions are able to use MSC/NASTRAN, MCS/DYTAN, MSC/EMAS, etc., as a black box together with new C or FORTRAN-source codes to perform extensive test series. Based on these results MSC should make a decision whether or not to implement new numerical procedures in general purpose software MSC/NASTRAN, MSC/DYTRAN, or MSC/EMAS.

REFERENCES

[1] R. RAUTMANN (Ed.), Approximationmethods for Navier-Stokes-Problems, Lecture Notes in Mathematics, 771, Springer Berlin, Heidelberg 1980

[2] U. A. SOLONIKOW, A. V. KASHIKOW, Existence Theorems for the Equations of Motion of a Compressible Viscous Fluid, Ann. Rev. of Fluid Mechanics 13, 79-95, (1981)

[3] H. LOMAX, U. B. MEHTA, Some Physical and Numerical Aspects of Computing the Effects of Viscousity and Fluidflow, Computational Methods in Viscous Flows, Volume 3, Pineridge Press, 1984

[4] H. OERTEL jr., M. BÖHLE, Strömungsmechanik II, Methoden und Phänomene, Springer Berlin, Heidelberg 1993

[5] E. LAURIEN, H. OERTEL jr., Grundzüge numerischer Methoden der Strömungsmechanik, Institutsbericht Nr. 93-4, Institut für Strömungsmechanik, TU Braunschweig, 1993

[6] N. GILBERT, Numerische Simulation der Transition von der laminaren in die turbulente Kanalströmung, Dissertation Universität Karlsruhe (TH), DFVLR-Forschungsbericht 88-55, 1988

[7] M. STOYNOV, B. L. ROZHDESTVENSKY, J. DELFS, E. LAURIEN, Stability and Efficiency of a Spectral Method for Compressible Boundary-Layer Transition and Turbulence Simulation, Report No. 92-14, Institut für Strömungsmechanik, TU Braunschweig 1992

[8] E. LAURIEN, J. DELFS, E. BOHNSACK, A Spectral Method for the Numerical Simulation of Compressible Boundary-Layer Transition, ZAMM 73, T556-T557, (1993)

[9] L. BREVDO, Instabile Wellenpakete in der Blasiusschen Grenzschichtströmung, ZLR-Forschungsbericht 92-02, Habilitationsschrift TU Braunschweig 1993

[10] J. DELFS, ZLR-Forschungsbericht 93-20, Dissertation TU Braunschweig, 1993

[11] B. MANDELBROT, On the geometry of homogeneous turbulence, with stress on the fractial dimension of iso-surfaces of scalars, J. Fluid Mech., Vol. 72, part 2, pp. 401-416, (1975)

[12] K. R. SREENIVASAN, C. MENEVEAU, The fractal facets of turbulence, J. Fluid Mech., Vol. 173, pp. 357-386, (1986)

[13] K. R. SREENIVASAN, Fractals and Multifractals in Fluid Turbulence, Annu. Rev. Fluid Mech. 23:539-600, (1991)

[14] R. RAMSHANKAR, Mixing in temporally developing shear layers: the multifractial approach, Proc. Forum Chaotic Dyn. ASME Fluids Eng. Conf., La Jolla, Calif. (1989)

[15] J. ZIEREP, H. OERTEL jr. (Eds), IUTAM Symposium Göttingen 1988, Symposium Transsonicum III, Springer Berlin, Heidelberg 1989

[16] P. KUTLER, A Perspective of Theoretical and Applied Computational Fluid Dynamics, AIAA Journal, Vol. 23, (1985)

[17] H. KÖRNER, K. H. HORSTMANN, H. KÖSTER, A. QUAST, G. REDEKER, Laminarization of Transport Aircraft Wings - a German View, AIAA Paper 87-0085, (1987)

[18] W. KORDULLA, H. SOBIECZKY, Summary and Evaluation of the Workshop "Numerical Simulation of Compressible Viscous-Flow Aerodynamics", Artikel in [15]

[19] D. SCHWAMBORN, Simulation of the DFVLR-F5 Wing Experiment Using a Block Structured Explicit Navier-Stokes-Method, Artikel in [20]

[20] W. KORDULLA (Ed.), Numerical Simulation of the Transsonic DFVLR-F5 Wing Experiment, Volume 22, Notes on Numerical Fluid Mechanics, Vieweg Braunschweig, Wiesbaden, 1988

[21] D. SCHWAMBORN, P. STRYKOWSKI, H. OERTEL jr., Numerical Simulation and Physical Modelling of Transsonic Trailing Edge Flow, Artikel in [15]

[22] H. W. STOCK, W. HAASE, The Determination of Turbulent Length Scales in Algebraic Turbulence Models for Attached and Slightly Separated Flows Using Navier-Stokes Methods, AIAA-87-1302, (1987)

[23] H. Oertel, Jr., GAMM-Mitteilungen, Heft 1, 11-37, 1994